Supporting Information

Toyabe et al. 10.1073/pnas.1106787108

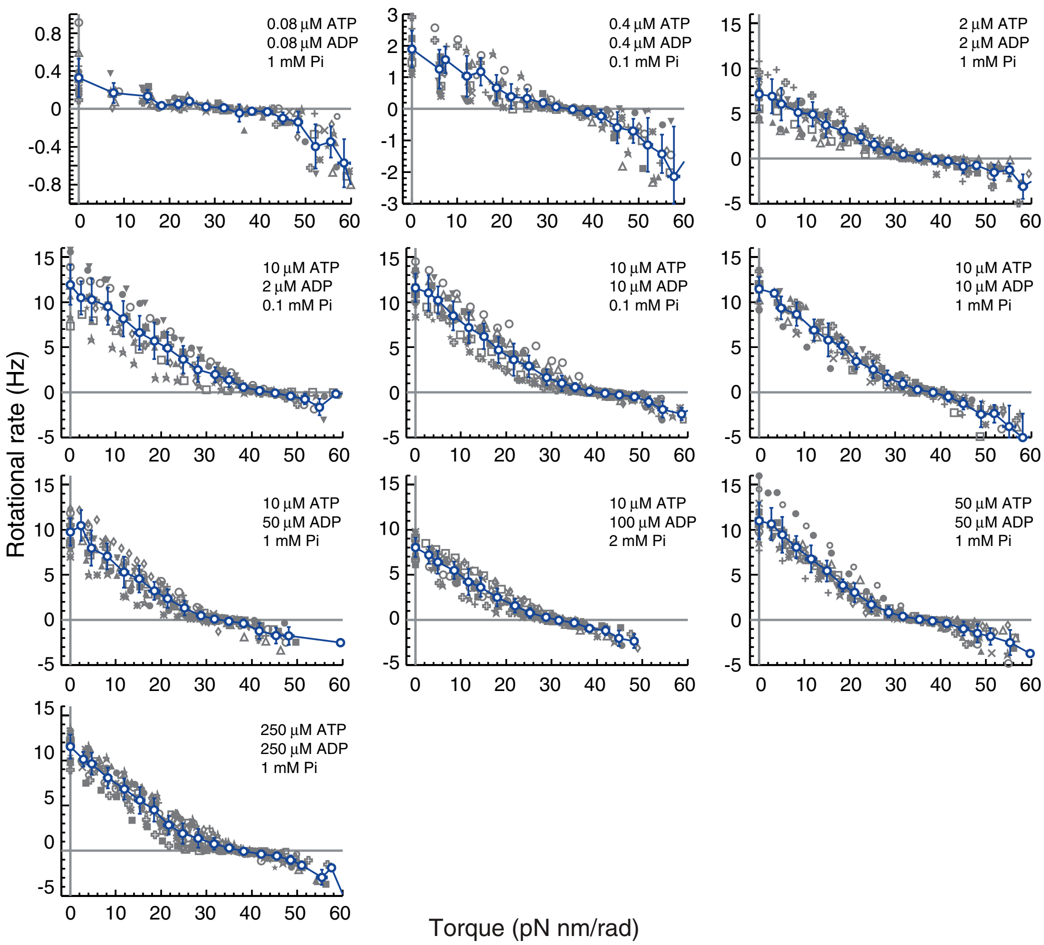

Fig. S1. Torque dependency of rotational rates of wild-type F_1-motor. Rotational rates of each molecule (gray). Different markers correspond to different molecules. Mean rotational rates (blue). Error bars correspond to SD.

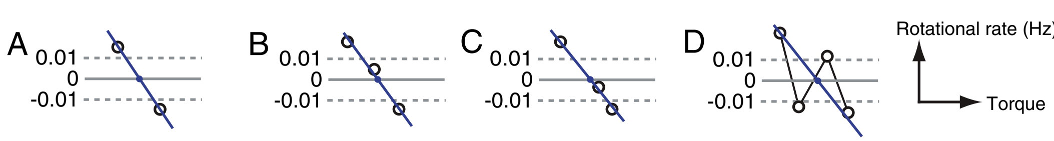

Fig. S2. Calculation of stall torque. We performed the following procedures to estimate the stall torque for each particle and then took the average under each condition. (*A*) Two data points closest to the horizontal axis were connected with a straight line. In the case that one or more data points have rotational rates less than 0.01 Hz (*B*, *C*) or that the data points show zigzag behavior (*D*), we fitted a straight line to data points including the outer points by the least-square method. We defined the stall torque as the intersection point of the horizontal axis and the fitted line. The results are summarized in Table S1 and Table S2.

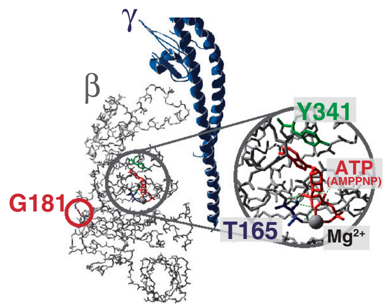

Fig. S3. We mutated one or more of the three amino acid residues in the hinge region (βT165S) and the ATP-binding site (βT165S and βY341W) of the β-subunit. Only $\beta_1\gamma_1$ subunits are shown for the simplicity. The structure is based on the mitochondrial F_1-ATPase (1).

1 Bowler MW, Montgomery MG, Leslie AGW, Walker JE (2006) How azide inhibits ATP hydrolysis by the F-ATPases. *Proc Natl Acad Sci USA* 103:8646–8649.

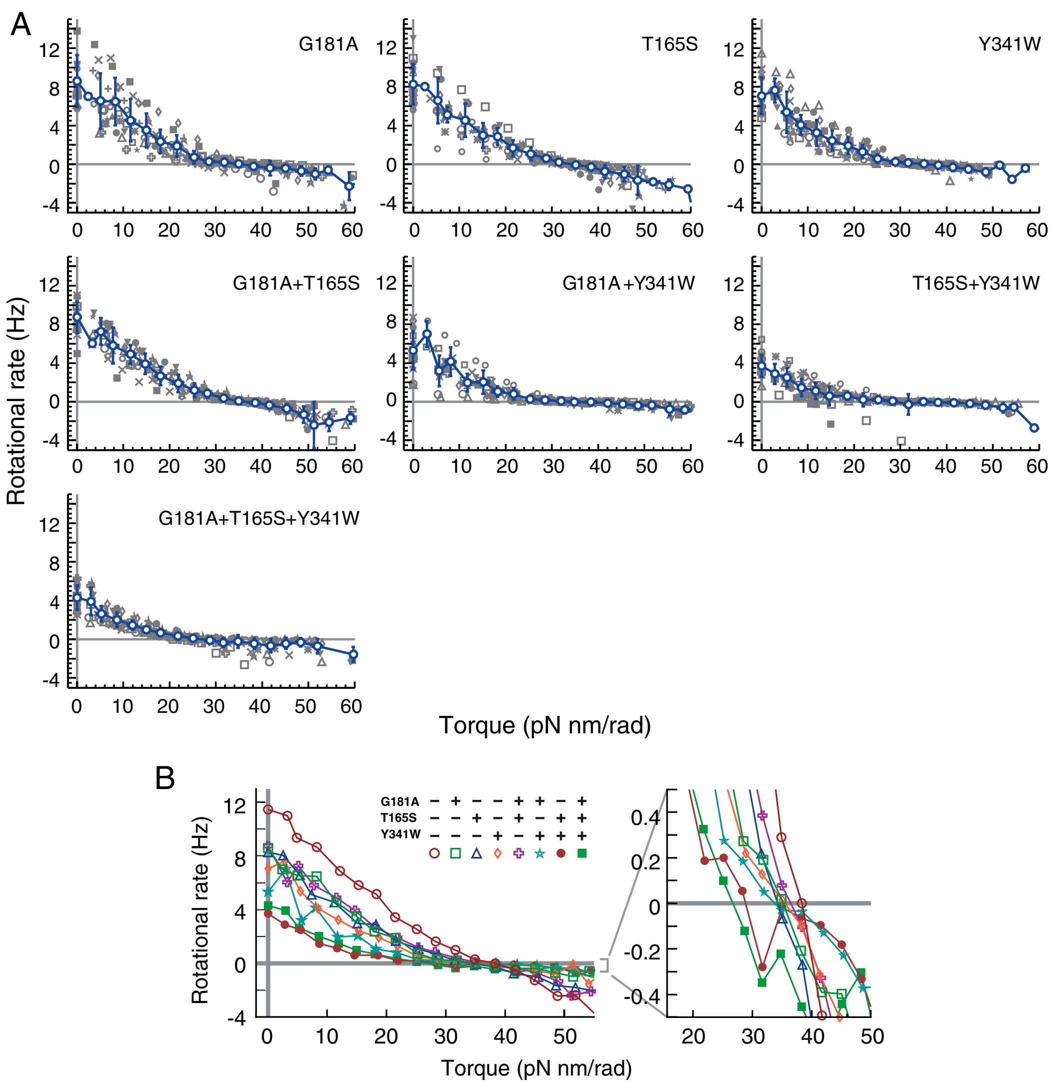

Fig. S4. (*A*) Torque dependency of rotational rates of mutated F_1-motor under 10 μM ATP, 10 μM ADP, and 1 mM P_i. Rotational rates of each molecule (gray). Different markers correspond to different molecules. Mean rotational rates (blue). Error bars correspond to SD. (*B*) Mean rotational rates of mutated F_1-motor under 10 μM ATP, 10 μM ADP, and 1 mM P_i.

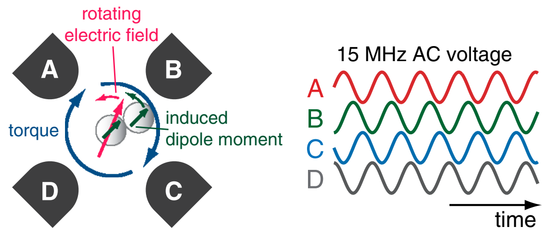

Fig. S5. Electrorotation method. Four electrodes are patterned on the bottom glass surface, with a spacing of 50 μm. A 15-MHz rotating electric field was generated at the center of four electrodes by applying sinusoidal voltages with a phase shift of $\pi/2$. Dielectric objects in this rotating electric field have a dipole moment rotating at 15 MHz. The phase delay between the electric field and the dipole moment resulted in the torque on the objects. Not to scale.

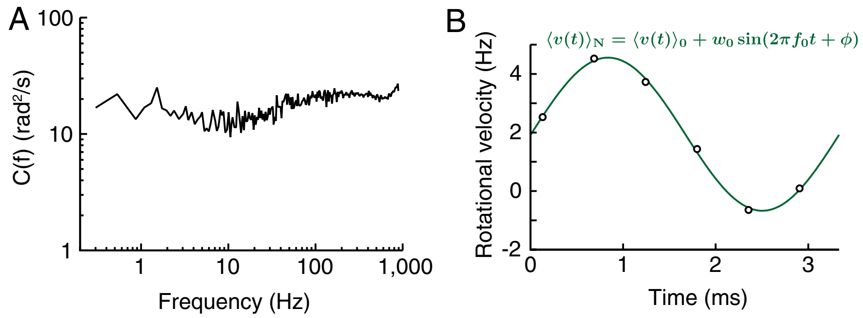

Fig. S6. Fluctuation and response of the rotational velocity of a typical example of a wild-type molecule under 0.4 μM ATP, 0.4 μM ADP, and 1 mM P_i. (*A*) Velocity fluctuation of an F_1-motor molecule in a frequency space. (*B*) The ensemble average of the rotational rate under a 300-Hz sinusoidal torque (circle) and the fitting curve by a sinusoidal function (solid line). The number of periods we averaged is 68,902. The amplitude of the torque is 9.9 pN nm/rad.

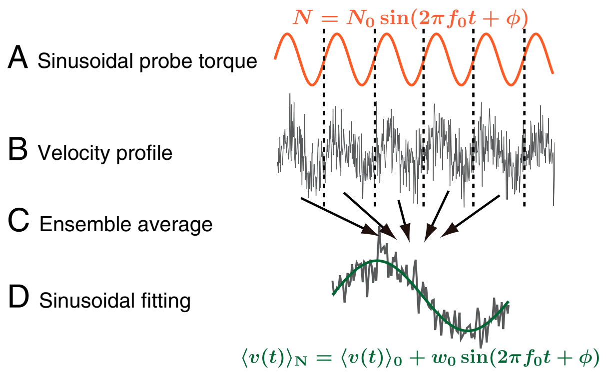

Fig. S7. Evaluation of response functions. (*A*) Sufficiently small sinusoidal external torque is applied. (*B*) Velocity profile is observed under this sinusoidal torque. (*C*) Ensemble average of the rotational rate for each period of the torque is taken. (*D*) Ensemble average is fitted by a sine curve to evaluate the phase and amplitude of the response function.

Table S1. Summary of the results for the wild type

	ATP	μM	10	10	0.08	0.4	2	10	50	250	10	10	
	ADP		2	10	0.08	0.4	2	10	50	250	50	100	
	P_i		100	100	1,000	1,000	1,000	1,000	1,000	1,000	1,000	2,000	
$\Delta\mu$	Pänke and Rumberg (1)	pN nm	88.4	81.8	72.4	72.4	72.4	72.4	72.4	72.7	65.8	60.2	
	Rosing and Slater (2)		89.5	82.8	73.4	73.4	73.4	73.4	73.5	73.7	66.8	61.2	
	Guynn and Veech (3)		94.4	87.8	78.4	78.4	78.4	78.4	78.4	78.7	71.8	66.2	
	mean		90.8	84.2	74.7	74.7	74.7	74.7	74.8	75.0	68.1	62.5	
W_{stall}	mean	pN nm	90.5	84.6	67.9	73.9	79.3	79.1	77.1	78.1	70.9	64.9	
	SD		3.2	3.2	8.7	4.9	5.1	4.8	4.2	4.3	4.2	2.3	
	SE		0.9	0.8	2.3	1.3	1.3	1.3	1.0	1.1	1.1	0.6	
ω_0	mean	Hz	12.4	11.6	0.33	1.90	7.12	11.5	11.0	11.5	9.84	8.03	
	SD		2.0	1.6	0.21	0.6	1.8	1.4	2.1	1.4	1.6	1.1	
	SE		0.6	0.4	0.05	0.2	0.5	0.4	0.5	0.3	0.4	0.3	
t test	ν	%	4.98	2.76	9.40	4.18	4.35	4.13	3.44	3.52	3.66	2.44	
	t		−0.39	−0.22	2.36	0.69	−2.04	−1.95	−1.11	−1.43	−1.27	−1.23	
	$P(>t)$ two-tail		71.0	84.2	4.2	74.0	10.6	12.1	33.4	20.0	27.8	32.7	Total
	n	• •	13	17	15	15	15	15	16	16	14	15	151
	$n_{2\sigma}$ • •	• •	2	0	1	1	1	1	1	0	1	2	10

Values of the standard free energy change $\Delta\mu°$ of ATP hydrolysis are different among literatures (1–3). We calculated $\Delta\mu$ on the basis of values reported in refs. 1–3 by a method developed by Krab and van Wezel (4). Data with stall torque larger than mean + 2 SD or smaller than mean − 2 SD were excluded from the analysis. The rotational rate in the absence of external torque is denoted by ω_0. To know if there is a significant difference between W_{stall} and $\Delta\mu$, we performed two-tail Welch's *t* test. For $\Delta\mu$, we regarded three values estimated based on refs. 1–3 as independent samples. The degree of freedom are ν and t, and the t-value of the *t* test, respectively. $P(>t)$ is the probability that a value larger than $|t|$ or less than $-|t|$ realizes. The number of the excluded samples is $n_{2\sigma}$.

1 Pänke O, Rumberg B (1997) Energy and entropy balance of ATP synthesis. *Biochim Biophys Acta* 1322:183–194.
2 Rosing J, Slater EC (1972) The value of $\Delta G°$ for the hydrolysis of ATP. *Biochim Biophys Acta* 267:275–290.
3 Guynn RW, Veech RL (1973) The equilibrium constants of the adenosine triphosphate hydrolysis and the adenosine triphosphate-citrate lyase reactions. *J Biol Chem* 248:6966–6972.
4 Krab K, van Wezel J (1992) Improved derivation of phosphate potentials at different temperatures. *Biochim Biophys Acta* 1098:172–176.

Table S2. Summary of the results for the mutants at 10 μM ATP, 10 μM ADP, and 1 mM P_i

Mutations	G181A		−	+	−	−	+	+	−	+	
	T165S		−	−	+	−	+	−	+	+	
	Y341W		−	−	−	+	−	+	+	+	
W_{stall}	mean	pN nm	79.1	75.0	73.8	74.9	77.1	76.0	69.0	63.7	
	SD		4.8	6.9	4.6	3.9	3.1	6.1	5.8	11.7	
	SE		1.2	1.8	1.2	1.0	0.8	1.6	1.4	2.9	
ω_0	mean	Hz	11.5	8.2	8.3	7.1	8.7	5.3	3.8	4.3	
	SD		1.4	2.2	2.2	2.0	1.7	2.1	1.2	1.3	
	SE		0.4	0.6	0.6	0.5	0.4	0.5	0.3	0.3	
t test	ν	%	4.13	8.35	3.95	3.31	2.81	5.51	4.93	13.4	
	t		−1.95	0.340	0.432	−0.0738	−1.20	−0.513	2.45	3.19	
	$P(>t)$ two-tail		12.1	91.9	68.6	94.8	32.4	63.0	5.82	0.69	Total
	n		15	15	15	15	15	15	16	16	122
	$n_{2\sigma}$		1	1	0	0	0	1	2	0	5

See the footnote of Table S1 for details.